Co-published by
Institute of Fluid-Flow Machinery
Polish Academy of Sciences
Committee on Thermodynamics and Combustion
Polish Academy of Sciences

http://www.imp.gda.pl/archives-of-thermodynamics/

Thermal performance of tubular heat exchangers with the discontinuous swirl-inducing conical baffle with opposite-oriented flow deflectors

Md Atiqur Rahman[a*]

[a] Department of Mechanical Engineering, Birla Institute of Technology, Mesra, Jharkhand 835215, India
*Corresponding author email: rahman.md4u@gmail.com

Received: 10.08.2023; revised: 29.12.2023; accepted: 01.04.2024

Abstract

An experiment was conducted to analyze a tubular heat exchanger's turbulent heat transfer characteristics. The heat exchanger was equipped with a newly designed perforated (rectangular) conical baffle plate consisting of two rectangular opposite-oriented flow deflectors with adjustable tilt angles. The baffle plate was installed at the entrance of the heat exchanger, resulting in a counter-swirling flow pattern downstream. Three baffle plates were installed along the flow direction with different pitch ratios (spacing between baffle plates divided by the diameter of the heat exchanger). The experiment examined the effects of pitch ratio (ranging from 0.6 to 1.2), deflector tilt angle (ranging from 30° to 50°) and Reynolds numbers (ranging from 16 500 to 30 000) on the heat transfer performance. The results showed that the pitch ratio and tilt angle significantly affected the performance of the heat exchanger. In particular, a configuration with a tilt angle of 30° and a pitch ratio of 1 resulted in an average improvement of 26.9% in the heat exchanger's performance compared to a heat exchanger without a conical baffle plate under similar operating conditions.

Keywords: Inclination angle; Recirculation; Rectangular deflector; Flow resistance; Swirl flow; Thermo-fluid performance

Vol. 45(2024), No. 2, 195–204; doi: 10.24425/ather.2024.150865

Cite this manuscript as: Rahman, M.A. (2024). Thermal performance of tubular heat exchangers with the discontinuous swirl-inducing conical baffle with opposite-oriented flow deflectors. *Archives of Thermodynamics*, 45(2), 195–204.

1. Introduction

Heat exchangers play a crucial role in various industries' thermal systems, making the use of heat transfer enhancement techniques essential for energy efficiency. These techniques have been widely implemented in refrigeration, automotive, process, and solar air heater systems to reduce energy consumption and operating costs [1–4]. Turbulators, or vortex/reverse flow devices, are commonly used in HT (heat transfer) engineering to improve heat and momentum transfer. By promoting vortex flow and boundary dissipation, turbulators enhance heat transfer coefficients and increase convection at the tube's surface. This is achieved by reducing the cross-sectional flow area, increasing velocity, and creating a higher temperature difference. These deflectors, when strategically placed in the flow field [5], can generate longitudinal swirl flow and can be referred to as swirl generators/promotors, which may be continuous, e.g. twisted tapes [6], or discontinuous [7]. A few of the literature showing the effect of deflector are discussed below.

Nomenclature

A – duct's cross-sectional area, m^2
A_c – duct area of cross-section, m^2
A_i – total heat transfer surface area, m^2
A_p – copper tube heat transfer surface area, m^2
BR – blockage ratio,
c_p – specific heat of air, kJ/(kg K)
d – outer diameter of copper tube, m
D – test section inner diameter, m
E – area (cross-sectional) of the test section, m^2
f – friction factor
h_m – convective heat transfer coefficient, $W/(m^2 K)$
H – height ratio, $= H_1/H_2$
j – Colburn factor
k_p – thermal conductivity of Plexiglas, W/(m K)
k_t – thermal conductivity of copper tube, W/(m K)
L – duct length, m
Nu – Nusselt number
p – distance between consecutive baffle plates, m
PEC – performance evaluation criterion
Pr – Prandtl number of air
PR – pitch ratio
Q – air side heat transfer rate, W
Re – Reynolds number
t – average temperature, °C
T – temperature, °C
TEF – thermal enhancement factor

Greek symbols

α – tilt angle (angle between the deflector and baffle plane), °
Δp – pressure drop in test section, Pa
Δp_o – pressure drop at orifice plate, Pa
Δt_{lm} – LMTD of test section
λ – thermal conductivity of air, W/(m K)
μ – dynamic viscosity of air, Pa s
v – average velocity, m/s
ρ – density, kg/m^3

Subscripts and Superscripts

a – local
in – inner
out – outer
w – wall

Abbreviations and Acronyms

CDBP– conical deflector baffle plate
HT – heat transfer
HX – heat exchanger
LMTD– logarithmic mean temperature difference
TEF – thermal enhancement factor
VG – vortex generator

Yaningsih et al. [8] conducted an experimental study to investigate the impact of a louvered strip insert's slant angle (α) on HT and f (friction factor). We examined slant angles of 15°, 20° and 25° at Reynolds number (Re) ranging from 5300 to 17 500. We also included a plain tube for comparison purposes. The results revealed that the louvered strip insert significantly enhanced HT and f compared to the plain tube, with increases of up to 77.02% and 3.35 times, respectively. Moreover, the results indicated that HT and f increased as the slant angle increased. The highest slant angle demonstrated the most favourable thermal enhancement factor (TEF) with a value of 1.12.

Bartwal et al. [9] investigated a novel geometric insert called circular rings with wire net inserts as HT enhancement devices. Three wire net grades (G = 4, 9, and 16) and three PRs (pitch ratio – p/D) of 2, 3 and 4 are chosen to investigate their impact on HT, f and TEF. Turbulent airflow with Re between 5 000 to 40 000 is used as the working fluid. The results show significant improvements in HT and pressure drop (Δp) in the test section compared to a smooth tube. Results showed that the highest TEF of approximately 3.35 is achieved for PR = 2 and G = 16. An extreme of 2.84 for TEF is obtained for PR = 3 and G = 9.

Ibrahim et al. [10] performed numerical investigations of the effectiveness of using conical rings as turbulators for enhancing heat transfer. Conical inserts were placed inside a tube, and the performance of three different configurations (convergent, convergent-divergent, and divergent) was analyzed. The study focused on air as the working fluid and Re between 6 000–25 000. Varying diameter ratios and pitch ratios were tested. Results showed that the Nu (Nusselt number) and f rose as the conical ring diameter and pitch ratio declined. Compared to a plain tube, the average Nu values achieved were significantly higher with the convergent, convergent-divergent and divergent ring arrays, with enhancements of 330%, 419% and 765%, respectively. The best overall performance was observed for the divergent ring with a diameter ratio of 0.4 and PR of 2 at the Reynolds number of 6000, achieving an enhancement in tube efficiency of 1.291.

Nalavade et al. [11] conducted experimental and numerical investigations of the effect of unique flow divider-type turbulators on the characteristics of f and HT for airflow inside a heated tube. The tests were conducted with Re between 7 000 and 21 000. The parameters studied included PR (p/D = 0.54, 0.72 and 1.09) and a twist angle 90°. These novel turbulators created additional turbulence near the tube wall, effectively disrupting the thermal boundary layer. Both experimental and numerical results showed that the HT rate, f and TEF increased with decreasing PR of the turbulators. This enhancement is attributed to the fluid displacement from the central core region towards the tube walls caused by the flow divider-type turbulator. Additionally, computational simulations were utilized to examine the impact of varying the twist angle of the turbulator, revealing that the Nusselt number increased by approximately 1.33–1.46 times and 1.43–1.60 times for angles of 45° and 30°, respectively.

Hassan et al. [12] experimentally examined a novel square turbulator tape with three square fins' design in a double-tube heat exchanger (HX). The inner copper tube side had diameters of 0.022 m, while plexiglass shells had diameters of 0.054 m, respectively. It was found that plummeting the width of fins augments the HT rate. The experimental results exhibit that the square-cut turbulator with a width of 0.25 cm resulted in a 271.7% increase in Nu number values, a 117.6% increase in total convective heat transfer coefficient (h_m), and a TEF of 2.9.

Lamlerd et al. [13] studied the impact of circular-ring tabulators on the HT characteristics of a steam generator. The tabulators have a tilt angle (α) of 45° with blockage ratio (BR) of 0.20 mm. The researchers investigated length ratios (LR) between 25% to 100%, PR of 1.0 to 4.0, and water flow rates of 12–36 l/h. Waste lubricating oil was utilized as the heat source to generate steam. The findings demonstrate that HX with circular-ring inserts outperforms a smooth tube in terms of steam rate (6.88–10.35% improvement), vapour quality (x) (0.21– 0.92 improvement), heat transfer (1.27–1.55 times improvement) and thermal efficiency (0.46–0.68 improvement).

Jayranaiwachira et al. [14] experimentally studied a heat exchanger equipped with louvered curved-baffle (LCB) vortex generator (VG). The study measured HT and Δp of air flowing through the tube at different Re ranging from 4760 to 29 300. LCB VGs have an attack angle of 30° arranged in a V-shape on two tape sides. The results showed that the LCB-inserted tube had significantly higher Nu and f compared to the plain tube. Additionally, Nu and f increased as the PR and tilt angle α decreased. LCB VGs increased Nu and f by 4.66 times and 39.37 times, respectively. The highest TEF was observed when the LCB had a PR of 1, $\alpha\ \theta$ of 45° and lower Re.

Promvonge et al. [15] investigated the effectiveness louver-punched V-baffle (LPVB) VG in improving thermal performance in a solar HX duct with air as the working fluid at Re ranging from 5 300 to 23 000. LPVBs with an α = 45° were placed on the heated wall of the duct. The investigation focused on determining the optimal PR and louver angles and exploring the impact of different relative louver sizes. The results showed that the LPVB with louver angles greater than 0° significantly reduced solid-baffle friction loss, although heat transfer was slightly lower. The LPVB with a relative baffle pitch of 1.5 and a louver angle of 45° demonstrated the best performance in the first part of the investigation, while the LPVB with a relative louver size of 0.9 performed the best in the second part.

Promvonge et al. [16] experimentally investigated the HT characteristics of a circular tube equipped with conical nozzles and a swirl generator. The conical nozzles, serving as turbulators and reverse flow generators, were placed in a modelled pipeline where the air was used as the working fluid. Different arrangements of the conical nozzles were tested, with three PR of 2.0, 4.0 and 7.0 in each run. Additionally, a snail design was employed to induce swirling flow at the tube inlet. Results showed significant improvements in heat transfer rate when using either the conical nozzles or the snail, with increases of approximately 278% and 206%, respectively, compared to a plain tube. Combining the conical nozzles with the snail resulted in a maximum HT rate enhancement of 316%.

Samruaisin et al. [17] experimentally investigated the effects of V-shaped delta-wing baffles on TEF of a circular tube. The baffles with different numbers of wings (4, 6 and 8) were compared. Various PR (p/D = 2.0, 2.5 and 3.0) were used to fit the V-shaped delta-wing baffles inside the tube. These baffles created both recirculation/reverse flow behind the solid baffle and longitudinal vortex flow behind the V-shaped wing. The V-shaped winged baffles with 8 wings showed higher HT rates by promoting the development of reverse and vortex flows, allowing for better fluid mixing. The Nu enhancement ranged from 97% to 105.6% for wings number N = 4, 105.8% to 127.8% for N = 6, and 114.8% to 138.9% for N = 8. The V-shaped winged baffles with 8 wings also created additional multi-vortex flows, contributing to fluid mixing and increased heat transfer. Lower pitch ratios increased turbulent intensity and led to a higher HT rate, with a Nusselt number increase of up to 118.26% to 151.3% compared to a tube with a pitch ratio of 2.0. Baffles with 8 wings and a pitch ratio of 3.0 had a maximum aerothermal performance factor (APF) of 1.01, indicating potential energy savings at low Reynolds numbers (Re ≤ 6 000).

Durmuş [18] experimentally investigated a swirl generator in the form of a snail attached at the entrance of a concentric double-pipe HX inner pipe. In the experimental setup, cold air was directed through the inner pipe while hot water flowed through the annulus. The study examined the impact of the snail on HT and Δp in both parallel and counter-flow configurations. The results were presented as a correlation between Nu, Re, Pr and the swirling angle. The highest enhancement, up to 120% in Nu, was observed in the counter-flow configuration with a swirling angle of 45°. Although the snail-induced swirl flow caused a slight increase in Δp, this was irrelevant compared to the improvement in HT efficiency.

Rahman and Dhiman [19,20] developed a novel tubular heat exchanger with axial flow and tested several configurations to enhance its heat transfer efficiency. They employed circular perforated plates with trapezoidal air deflectors at different angles (α) to induce turbulence in the air duct surrounding the hot water tube bundle. The plates, spaced evenly but with varying pressure ratios, were found to significantly improve the thermal and fluid performance of HX when inclined at 50° and with a pressure ratio of 1.4. They further studied the geometric constraint by replacing the trapezoidal deflector with rectangular openings with one deflector [21] or two opposite-oriented flow deflectors [22] on the HT and flow characteristics. It was found that using a single flow deflector resulted in a 41.49% enhancement in TEF while incorporating two flow deflectors with opposing orientations only achieved 0.19 times the thermal effectiveness equated to a HX without a baffle plate. Using opposite-oriented diverters improved heat transfer rates and increased pressure drop (Δp). Rahman [23] further replaced perforated flat circular baffles with flow diverters in an HX to a conical baffle plate (CBP), resulting in a 22% improvement in thermal effectiveness. In another experiment, multiple (sixteen) rectangular deflectors [24] were used as flow deflectors, leading to a 1.17 enhancement in thermal effectiveness for a PR of 1 and an angle (α) of 30°. Furthermore, the use of triangular blinds [25] as flow deflector baffles showed additional improvement in the HT efficiency of HX.

Habet et al. [26] studied the effects of different angles of tilt (0°, 30°, 45° and 60°), and ratios of perforation (ranging from 10% to 40%) were investigated in a rectangular channel with an aspect ratio of 3:1. The upper and lower surfaces of the channel were insulated. They were exposed to a uniform heat flux. The research focused on Reynolds numbers ranging between 12 000 and 42 000. The results showed that the best HT enhancement and significant changes in friction factor occurred when the baffles were tilted at a 0-degree angle and had a perforation ratio of

10%. When the angles of tilt and perforation ratios were lower, the heating surfaces experienced stronger reattachment and recirculating flow, leading to increased HT and a Nu ratio of 2.6. The configuration that yielded the highest TEF of 0.7 was achieved with a 60-degree angle of tilt and a perforation ratio of 10% at the Reynolds number of 12 000.

The aforementioned literature reveals that the implementation of swirl promoters within a heat exchanger yields improved fluid mixing. Consequently, this leads to heightened heat transfer capabilities as the fluid and heat transfer surfaces have more substantial contact, resulting in elevated heat transfer coefficients. Additionally, the incorporation of swirl flow reduces fouling in heat exchangers by preventing the accumulation of deposits on high-temperature surfaces. This is primarily achieved by the continuous agitation of the fluid, which effectively washes the surfaces and facilitates the removal of unwanted elements. These two factors collectively contribute to a higher thermal efficiency within the heat exchanger. The heat exchanger can achieve the desired heat transfer objectives with minimal energy input, resulting in energy savings and an overall increase in system effectiveness. Another advantageous outcome of swirl flow is its capacity to enable the design of more compact HX. The enhanced heat transfer capabilities achieved through the swirling motion allow for smaller heat transfer surfaces or reduced heat exchanger sizes, optimizing space utilization. Furthermore, the implementation of a swirler can also address the issue of stagnation zones within the heat exchanger. By promoting a more uniform distribution of temperature, the swirler helps eliminate areas where fluid movement is limited. This feature is particularly crucial in applications where maintaining a consistent temperature profile, such as thermal processing or heating/cooling systems, is critical.

In recent studies, scientists have been exploring novel methods to improve the transfer of heat and reduce pressure drop in devices that induce rotational movement. These advancements include the utilization of coiled structures [27], twisted strips [28], and perforated cone-shaped rings [29]. Different perforation patterns, such as triangles [25], rectangles [22], circles and trapezoids [19], have been experimentally examined to find the most effective way to enhance heat transfer or reduce pressure variations. Novel baffle plate designs like conical [18], and conical with perforation [23] have been studied. However, the understanding of utilizing multiple flow deflectors [21] on baffle plates and the deflector orientation [24] on thermal-hydraulic performance is limited in the current literature. This study aims to bridge these knowledge gaps by developing and evaluating a unique design for a device that induces discontinuous swirling motion. Our approach involves incorporating opposing flow deflectors on conical baffle plates to induce swirling motion and turbulence in the fluid.

The primary objective of this research is to develop and test a novel perforated conical baffle plate capable of producing a swirl, which aims to manipulate the flow. This device achieves its purpose by utilizing opposite-oriented rectangular deflectors mounted on each conical baffle plate (CDBP) to induce a counter-swirl motion and turbulence. The flow deflectors are strategically positioned at a slant length of 15 mm from the apex of the conical baffle plate. Three successive baffle plates are located within HX at regular intervals to facilitate flow reversal, extending residual air time within HX and disrupting the thermal boundary layer, causing air-side HT augmentation.

The study investigates the influence of two key factors: the ratio of HX diameter to the distance between adjacent baffle plates (PR) and the inclination angle (α) in circular ducts for heat transfer (HT) and friction factor (f). The PR values are considered in the range from 0.6 to 1.2, while the tilt angle varies between 30° and 50°. The experimental analysis maintains consistent conditions, with Reynolds numbers ranging between 15 000 and 30 000. Further performance comparison in terms of TEF is done between HX with and without baffle plate under similar operating parameters.

2. Materials method

2.1. Experimental configuration

The experiment was carried out within an open-loop experimental system, as Rahman and Dhiman extensively described in [19,20]. The loop consisted of a circular duct linking a 4 kW blower to a settling tank, with the inclusion of an orifice flow meter in this pipeline. Following the straightener, a channel was utilized, comprising a calm segment measuring 1.3 m, a test segment measuring 0.6 m, and an exit measuring 0.3 m. The test channel, portrayed in Fig. 1, was constructed using plexiglass material characterized by low thermal conductivity, featuring a channel diameter (D) of 19 cm, a length (L) of 60 cm and a thickness of 0.5 cm.

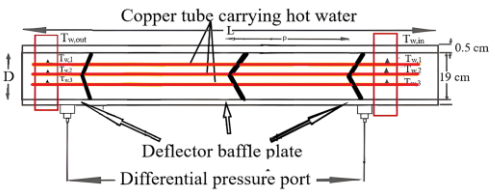

Fig. 1. Test section.

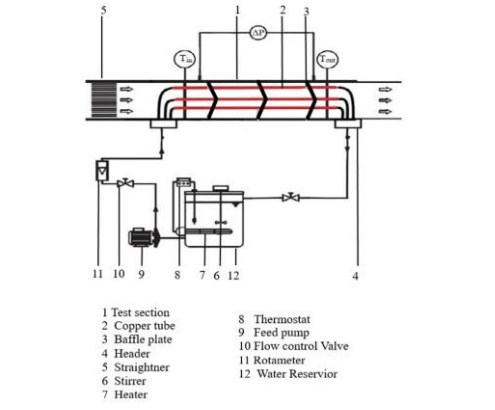

Fig. 2. Hot water loop.

Inside the test section, three conical baffles, each having a thickness of 5 mm and fabricated using 3D printing technology, were placed at equal intervals. Further details regarding these baffles will be elaborated later in this section. A nondimensional parameter, known as pitch ratio (PR = p/D) was investigated at four specific values: 0.6, 0.8, 1 and 1.2. The test section was wrapped with cotton wool to minimize heat loss and covered with 8 mm urethane foam. Further, five copper tubes (DHP 12 200) with an outer diameter (d) of 1 cm and a thickness of 1 mm were arranged in a circular array, with one at the centre and the other four at a circular distance of 5 cm from the centre of the baffle plate. To calculate h_m (Eq. (5)) of air, the tube average surface temperature at the inlet ($T_{w,in}$) and outlet ($T_{w,out}$) is measured using ten J-type thermocouples attached to NI-9213 DAQ card with a resolution of ± 0.02°C with digital readout using LabView software. Two additional thermocouples ($T_{a,in}$ and $T_{a,out}$) are employed at the test section's air inlet and exit. Also, Δp in the test section is measured using silicon microstructure pressure transducers (connected to an analogue-to-digital converter – ADC), board interface and RS 232 serial interface) with digital readout via Lab-View software.

A closed hot water loop was employed to provide heat to the test section, as illustrated in Fig. 2. The water was heated using an electrical heater with a power rating of 4 kW, whose temperature was then regulated by a thermostat in a reservoir. The heated water was circulated at a constant flow rate of 4 LPM (litres per minute) to a distributor using a 0.25 hp (0.18 kW) feed pump, a bypass valve and a rotameter. The temperature of this hot water was measured using PT100 and uniformly distributed to all the copper tubes within the test section.

Table 1. Experimental operating conditions [20].

Air-inlet temperature, °C	32.5 ± 0.5
Air-inlet velocity, m/s	7–13
Water-inlet temperature, °C	55–60
Water mass flow rate, kg/s	0.06

Table 2. The accuracies of the measurements [20].

Parameters	Accuracy
Air temperature-inlet, °C	± 0.5
Pressure drops, Pa	± 0.1
Water temperature-inlet, °C	± 0.5
Water flow rate, kg/s	± 0.003

During experimentation, the cold air from the atmosphere is sucked in using a blower which enters the test section after passing through a straightener. As it travels through the test section, it gains temperature, which is used in calculating h_m. Modifications are made to the airflow rate (constant Re) while maintaining a consistent water flow rate during the experiment to conduct a comparative analysis. The arrangement is then permitted to achieve a state of equilibrium, at which point the air and surface temperatures of the copper pipes in the test section are measured.

Table 1 provides a condensed overview of the testing criteria, while Table 2 demonstrates the determination of instrument precision by utilizing the root mean sum square method. The potential maximum uncertainty associated with the variables Re, v, f and Q is estimated to be ± 3.25, ± 5, ± 5.34 and ± 5%, respectively [30].

2.2. Baffle plate and tube arrangement

The CDBP of fixed height (h = 5 cm) with a geometry angle of 28° as seen in Figs. 3(a)–3(c) comprises five tube configurations. The central configuration is surrounded by four tubes arranged in a circular pattern, positioned 4 cm away from the centre of the conical plate. Four regularly spaced rectangular openings of $7d \times 1.5d$ are integrated into the baffle plate with a distance of $1.5d$ from the centre of the baffle to ensure smooth airflow. Two deflectors of the same dimensions ($3.5d \times 1.5d$) are oppositely oriented to each other and are fixed on each rectangular opening at a tilt angle (α). One deflector named FD1 is directed towards the tube bundle. At the same time, FD2 is directed towards the test section wall. This arrangement generates two counter-swirl flow currents between the baffles, intending to generate counter-rotational airflow within the test section, enhancing mixing and heat transfer and increasing Δp. The turbulent intensity, vortex formation and flow rotation can be manipulated by adjusting the baffle PR (0.6, 0.8, 1 and 1.2) and deflector tilt angles (30°, 40°

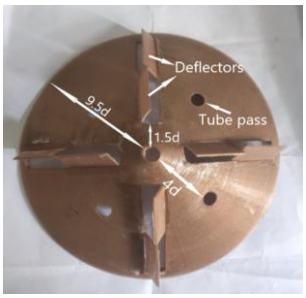

Fig. 3(a). Conical deflector baffle plate.

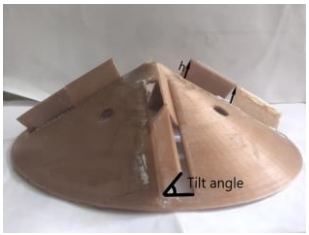

Fig. 3(b). Tilt angle.

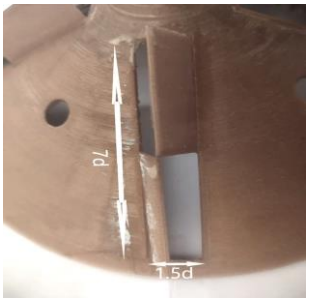

Fig. 3(c). Deflector details.

and 50°). The baffle plate is intentionally placed at the inlet to generate discontinuous swirl flow downstream and support the tube bundle.

2.3. Design parameters

The following design parameters are defined below, the pitch ratio [19,20]:

$$\mathrm{PR} = \frac{p}{D}, \tag{1}$$

and the blockage ratio [21,22]:

$$\mathrm{BR} = \frac{S}{E}, \tag{2}$$

where: $S = E$ – (4 × area of the rectangular perforation), α – deflector tilt angle.

This study focused on investigating the impact of different tilt angles on three specific configurations of counter-directional deflector profiles on CDBP. The tilt angles considered were 30°, 40° and 50°, while the duct maintained a constant blockage ratio of 0.70 and a longitudinal flow. Furthermore, the experiment was replicated by altering the PR between 0.6, 0.8, 1 and 1.2. Comparisons were made between the obtained data to analyze how the PR, α, influenced the relative j and f values, and PEC (defined as PEC = $(j/j_0)/(f/f_0)^{1/3}$).

2.4. Data aggregation

Cao's technique [31] is used to evaluate h_m:

$$h_m = Q/A_p \Delta t_{lm}, \tag{3}$$

where:

$$Q = c_p \rho v A_c \left(T_{a,out} - T_{a,in}\right), \tag{4}$$

$$v = \sqrt{2\Delta p_o/\rho}, \tag{5}$$

and Δt_{lm} is estimated as

$$\Delta t_{lm} = \frac{\left(t_{w,in} - T_{a,in}\right) - \left(t_{w,out} - T_{a,out}\right)}{\ln\left(t_{w,in} - T_{a,in}\right)/\left(t_{w,out} - T_{a,out}\right)}. \tag{6}$$

The average surface temperature of the copper tube wall is calculated by averaging the surface temperature at the inlet ($t_{w,in}$) and the outlet ($t_{w,out}$):

$$t_{w,in} = \left[\frac{\sum_1^5 T_{w,i} A_i}{A_p}\right]_{in}, \qquad t_{w,out} = \left[\frac{\sum_1^5 T_{w,i} A_i}{A_p}\right]_{out}, \tag{7}$$

where i at the inlet refers to the thermocouples 1–5, while i at the exit refers to thermocouples 6–11, A_i is the HT area of an individual tube and T_w represents individual copper tube surface temperature. The average Nu, f and j are described as:

$$\mathrm{Nu} = \frac{h_m D_h}{\lambda}, \tag{8}$$

$$f = \frac{2\Delta p D}{\rho v^2 L}, \tag{9}$$

$$j = \frac{\mathrm{Nu}}{\mathrm{RePr}^{1/3}}. \tag{10}$$

From Eqs. (4) and (6):

$$h_{c,m} = \frac{c_p \rho v A_c \left(T_{a,out} - T_{a,in}\right)}{A_p \Delta t_{lm}}. \tag{11}$$

Dimensionless factors like (j/j_0), (f/f_0) and PEC were used, where f_0 and j_0 serve as benchmarks and represent the test section without CDBP [22,23].

3. Results and discussion

3.1. Heat transfer augmentation

Figure 4 displays the relative Coburns factor (j/j_0) for three different deflector tilt angles (α = 30°, 40° and 50°), investigated at varying Re and pitch ratios (PR). The j/j_0 values for CDBP first reduce with the rise in Re and then increase with the increasing Reynolds number until reaching a peak value, after which they decrease. A similar pattern is observed for all other α. Notably, CDBP with a smaller inclination angle (α = 30°) exhibits the highest relative j/j_0 values among the different inclination angles.

At a smaller inclination angle, the velocity of air entering the duct increases. This increase in velocity corresponds to higher eddy energy, which refers to the energy associated with random fluid motions. The presence of eddies generates convective cells on the tube surfaces, promoting faster heat transportation compared to laminar flow conditions. Moreover, eddies increase the effective surface area near the tube walls, enhancing heat transfer.

The narrowing passage of the airflow caused by the smaller α of the deflectors results in an inclined jet flow and swirl flow upon entering the test section. This swirling motion disrupts the boundary layer formation and improves heat transfer. It also enhances the flushing ability of the fluid on the duct side. However, at higher Reynolds numbers, the increased velocity can reduce residence time near the heat transfer surface, limiting effective heat exchange.

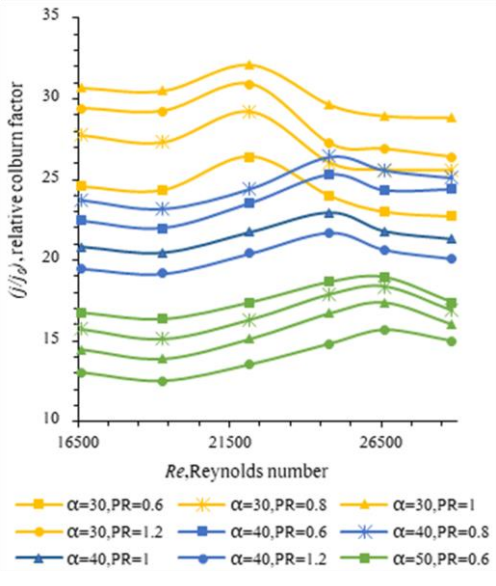

Fig. 4. Fluctuation in j/j_0 with Re.

Additionally, the flow may become highly turbulent, resulting in a thicker inertial sublayer that acts as a thermal resistance. Moreover, flow separation and recirculation zones can occur, creating quasi-stagnant regions that hinder heat transportation and reduce heat transfer performance. While it is generally assumed that higher Reynolds numbers lead to higher heat transfer rates, in these cases, factors such as reduced residence time, turbulence, flow separation and recirculation can actually decrease the heat transfer with the increasing Reynolds number. The optimized Reynolds number and pitch ratio for efficient heat transfer can be found in Fig. 5.

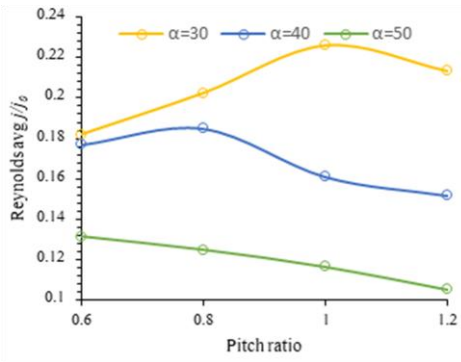

Fig. 5. Reynolds number averaged j/j_0 vs. PR.

The research conducted by Wang et al. [32] emphasized the significance of PR in relation to heat transfer enhancement. The study revealed that the downstream vortex flow increases as the spacing between down-wash baffle plates decreases. However, if the spacing is too small, the interaction between vortex flows becomes strong, resulting in vortex break-up and diminishing the heat transfer enhancement. On the other hand, larger spacing causes rapid separation of vortex flow from the boundary layer, leading to high-pressure losses. Consequently, it is crucial to determine an appropriate PR to optimize the heat transfer.

Figure 4 also demonstrates the relative j/j_0 based on the pitch ratio PR for different Reynolds numbers ranging from 16 600 to 28 800 at tilt angles (α) of 30°, 40° and 60°. The heat transfer performance peaks at a specific PR value for each tilt angle are shifted towards lower PR values as α increases. To further understand the impact of PR and α, the averaged values of relative j/j_0 are plotted in Fig. 6. The plot illustrates that the relative j/j_0 value varies with PR at each α, and the maximum j/j_0 represents the optimum combination of PR and α. Figure 6 guides determining the optimum combination, showing that decreasing α and increasing PR results in a higher heat transfer. Additionally, by referring to Fig. 6, it can be observed that a PR value of 0.6 and α of 50° yield the lowest heat transfer, while a PR value of 1 and α of 30° result in higher heat transfer.

3.2. Friction factor and thermo-fluid performance

The combination of two oppositely oriented deflectors creates counter-swirl flow, which constantly washes the tube bundle and test section wall, creating a larger air-surface interaction area, and hence a higher frictional loss. Figure 7 presents a graphical representation of the friction factor ratio (f/f_o) as a function of Re at different PRs. From a heat transfer perspective, it is evident that higher friction over the surface leads to increased heat transfer. However, this can also result in a rise in pressure drop due to friction. The f/f_o values exhibit a wide range for all PR at various α of the deflector.

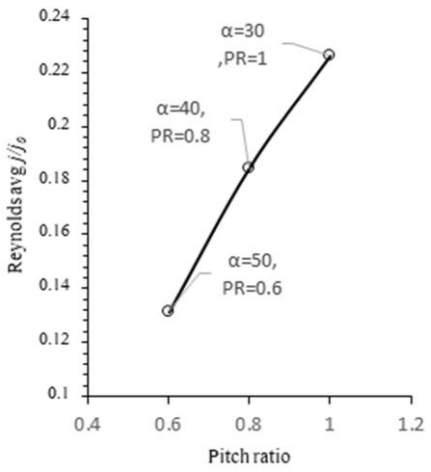

Fig. 6. Maximum Reynolds number averaged j/j_o values for different α.

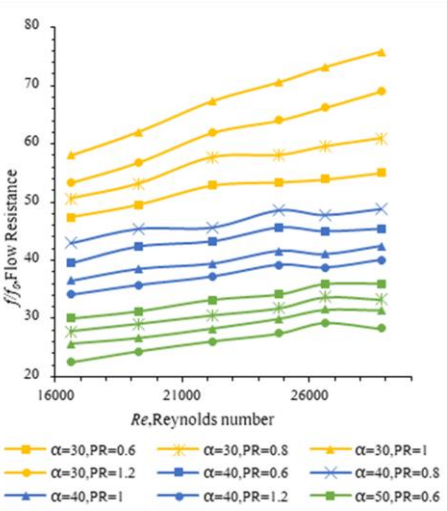

Fig. 7. Effect of Re on flow resistance (f/f_o)

The f/f_o values increase with Re, and the rate of increase remains consistent across all PRs. This indicates that the rise in friction from the entrance to the duct's exit follows a constant trend. The highest f/f_o value is observed at α = 30° but consistently decreases with increasing α.

To provide a more generalized observation, the Reynolds averaged f/f_0 values are plotted against PR for different α in Fig. 8. The trend in the graph is similar to that of Fig. 5, suggesting that a higher heat transfer leads to a higher frictional loss. The lowest recorded relative frictional loss is at PR = 0.6 for α = 30°. The maximum j/j_0 and minimum f/f_0 are tabulated in Table 3. Further, the minimum Reynolds number averaged f/f_o values obtained for different PRs are shown in Fig. 9.

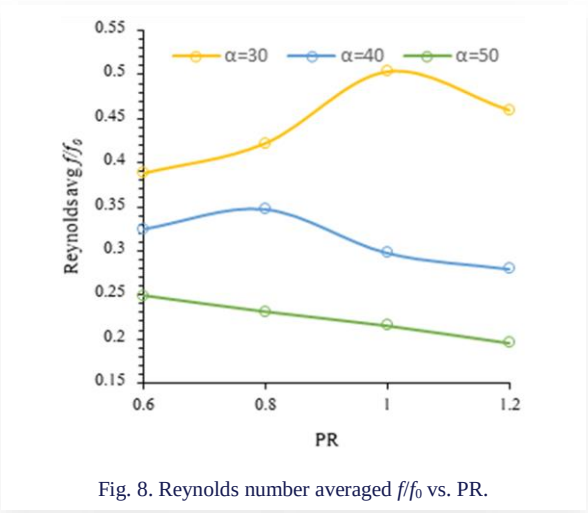

Fig. 8. Reynolds number averaged f/f_0 vs. PR.

Table 3. Maximum and mimimum value of relative j and f.

α	j/j_0		f/f_0	
	PR	Max value	PR	Min value
30°	1	0.503	0.6	0.38
40°	0.8	0.347	1.2	0.27
50°	0.6	0.24	1.2	0.19

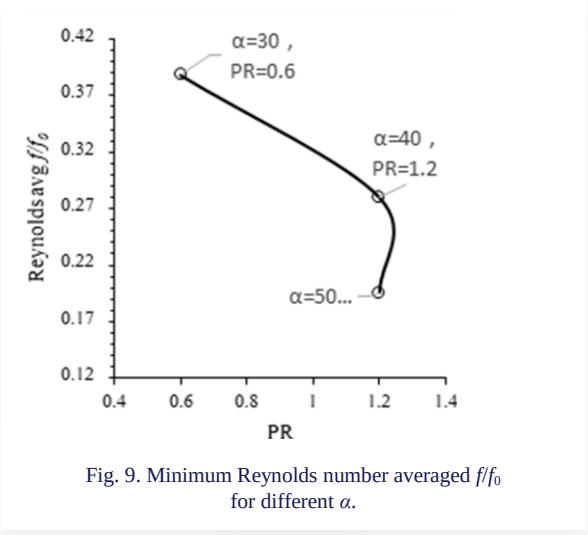

Fig. 9. Minimum Reynolds number averaged f/f_0 for different α.

The pressure drop of air flow between the entrance and exit of the duct is heavily influenced by the arrangement of baffle plates, the deflectors' tilt angle and the baffles' pitch ratios. To provide a visual representation of this relationship, Fig. 10 displays the plotted pressure drop values against different air volume flow rates. The figure clearly demonstrates that as the volume flow rate of air through the duct increases, the pressure drop also increases. Additionally, the slope of the pressure drop curve becomes steeper with higher pitch ratios. The figure also reveals that the slope of the pressure drop is most prominent at higher PRs, and it decreases as α increases. Another noteworthy observation is that the pressure drop is higher at a low inclination angle of the deflector (α = 30°), but it decreases as the inclination of the deflectors increases.

In Fig. 11, for a given Re range, the tilt angle of 30° gives the maximum PEC at PRs larger than 1, compared to larger angles. Smaller angles yield a higher heat transfer ability with comparatively low friction losses at larger PRs. A maximum of a 0.28 times increment in PEC is recorded using CDBP at α = 30° and PR = 1.

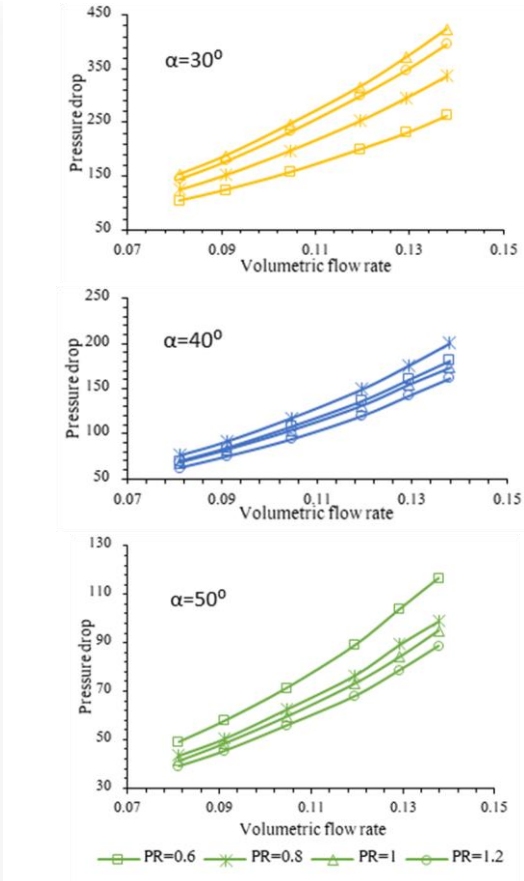

Fig. 10. Pressure drops for different α.

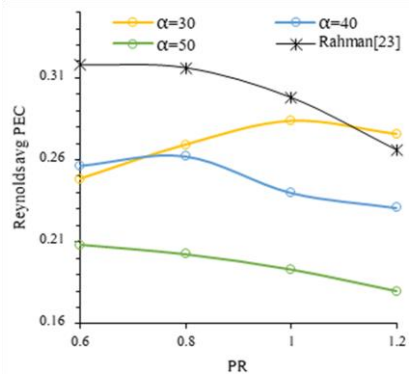

Fig. 11. Averaged PEC-value comparison.

Further comparison with the available literature on CDBP with a single deflector shows that employing an opposite-oriented deflector leads to an average decrement of 10% in PEC due to the relatively higher friction.

4. Conclusions

Upon comparing conical deflector baffle plate (CDBP) samples, it is noted that:

1. For the given Re range, the maximum average relative Colburn factor reduces with an increase in α, with maximum (j/j_0) value obtained at a lower α and then diminishes with the rise in α.
2. Re at which the maximum (j/j_0) is attained increases with an increase in the α value from 22 200 for $\alpha = 30°$ to 26 000 for $\alpha = 50°$.
3. The optimum PR to maximize j reduces with a rise in α from 1 for $\alpha = 30^o$ to 0.6 for $\alpha = 50^o$.
4. The flow resistance increases with an increase in Re.
5. The average PEC value achieves its maximum of 0.28 at $\alpha = 30°$ at PR = 1, and declines with the rise in α.

References

[1] Bergles, A. E., & Webb, R. L. (1985). Guide to the literature on convection heat transfer augmentation. *Advances in Enhanced Heat Transfer*, 43, 81–89.

[2] Shelare, S.D., Aglawe, K.R., & Belkhode, P. . (2022). A review on twisted tape inserts for enhancing the heat transfer. *Materials Today Proceedings*, 54, 560–565. doi: 10.1016/j.matpr.2021.09.012

[3] Poonpakdee, P., Samutpraphut, B., Thianpong, C., Chokphoemphun, S., Eiamsa-ard, S., Maruyama, N., & Hirota, M. (2022). Heat Transfer Intensification in a Heat Exchanger by Means of Twisted Tapes in Rib and Sawtooth Forms. *Energies*, 15, 8855. doi: 10.3390/en15238855

[4] Abed, N., & Afgan, I. (2020). An extensive review of various technologies for enhancing the thermal and optical performances of parabolic trough collectors. *International Journal of Energy Research*, 44, 5117–5164. doi: 10.1002/er.5271

[5] Dong, Z., Liu, P., Xiao, H., Liu, Z., & Liu, W. (2021). A study on heat transfer enhancement for solar air heaters with ripple surface. *Renewable Energy*, 172, 477–487. doi: 10.1016/j.renene.2021.03.042

[6] Barzegar, A., & Vahid, J.D. (2019). Numerical study on heat transfer enhancement and flow characteristics of double pipe heat exchanger fitted with rectangular cut twisted tape. *Heat and Mass Transfer*, 55, 3455–3472. doi: 10.1007/s00231-019-02667-1

[7] Nanan, K., Thianpong, C., Pimsarn, M., Chuwattanakul, V., & Eiamsa-ard, S. (2017). Flow and thermal mechanisms in a heat exchanger tube inserted with twisted cross-baffle turbulators. *Applied Thermal Engineering*, 114, 130–147. doi: 10.1016/j.applthermaleng.2016.11.153

[8] Yaningsih, I., Wijayanta, A. T., Miyazaki, T., & Koyama, S. (2018). Thermal hydraulic characteristics of turbulent single-phase flow in an enhanced tube using louvered strip insert with various slant angles. *International Journal of Thermal Sciences*, 134, 355–362. doi: 10.1016/j.ijthermalsci.2018.08.025

[9] Bartwal, A., Gautam, A., Kumar, M., Mangrulkar, C. K., & Chamoli, S. (2018). Thermal performance intensification of a circular heat exchanger tube integrated with compound circular ring–metal wire net inserts. *Chemical Engineering and Processing: Process Intensification*, 124, 50–70. doi: 10.1016/j.cep.2017.12.002

[10] Ibrahim, M.M., Essa, M.A., & Mostafa, N.H. (2019). A computational study of heat transfer analysis for a circular tube with conical ring turbulators. *International Journal of Thermal Sciences*, 137, 138–160. doi: 10.1016/j.ijthermalsci.2018.10.028

[11] Nalavade, S.P., Prabhune, C.L., & Sane, N.K. (2019). Effect of novel flow divider type turbulators on fluid flow and heat transfer. *Thermal Science and Engineering Progress*, 9, 322–331. doi: 10.1016/j.tsep.2018.12.004

[12] Hassan, J. H., & Hameed, V. M. (2022). Evaluate the hydrothermal behavior in the heat exchanger equipped with an innovative turbulator. *South African Journal of Chemical Engineering*, 41, 182–192. doi: 10.1016/j.sajce.2022.06.003

[13] Lamlerd, B., Bubphachot, B., & Chompookham, T. (2023). Experimental investigation of heat transfer characteristics of steam generator with circular-ring turbulators. *Case Studies in Thermal Engineering*, 41, 102549. doi: 10.1016/j.csite.2022.102549

[14] Jayranaiwachira, N., Promvonge, P., Thianpong, C., Promthaisong, P., & Skullong, S. (2023). Effect of louvered curved-baffles on thermohydraulic performance in heat exchanger tube. *Case Studies in Thermal Engineering*, 42, 102717. doi: 10.1016/j.csite.2023.102717

[15] Promvonge, P., Promthaisong, P., & Skullong, S. (2022). Heat transfer augmentation in solar heat exchanger duct with louver-punched V-baffles. *Solar Energy*, 248, 103–120. doi: 10.1016/j.solener.2022.11.009

[16] Promvonge, P., & Eiamsa-ard, S. (2006). Heat transfer enhancement in a tube with combined conical-nozzle inserts and swirl generator. *Energy Conversion and Management*, 47, 2867–2882. doi: 10.1016/j.enconman.2006.03.034

[17] Samruaisin, P., Rangsan M., Thianpong, C., Chuwattanakul, V., Maruyama, N., Hirota, M., & Eiamsa-ard, S. (2023). Enhanced Heat Transfer of a Heat Exchanger Tube Installed with V-Shaped Delta-Wing Baffle Turbulators. *Energies*, 16(13), 5237. doi: 10.3390/en16135237

[18] Aydın Durmuş, A., Durmuş, A., & Esen, M. (2002). Investigation of heat transfer and pressure drop in a concentric heat exchanger with snail entrance. *Applied Thermal Engineering*, 22(3), 321–332. doi: 10.1016/S1359-4311(01)00078-3

[19] Rahman, M.A., & Dhiman, S.K. (2023). Performance evaluation of turbulent circular heat exchanger with a novel flow deflector-type baffle plate. *Journal of Engineering Research*, 100105. doi: 10.1016/j.jer.2023.100105

[20] Rahman, M.A., & Dhiman, S.K. (2023). Investigations of the turbulent thermo-fluid performance in a circular heat ex-changer with a novel flow deflector-type baffle plate. *Bulletin of the Polish Academy of Sciences Technical Sciences*, 71(4). doi: 10.24425/bpasts.2023.145939

[21] Rahman, M.A. (2024). Effectiveness of a tubular heat exchanger and a novel perforated rectangular flow-deflector type baffle plate with opposing orientation. *World Journal of Engineering*. doi: 10.1108/WJE-06-2023-0233

[22] Rahman, M.A. (2023). Experimental Investigations on Single-Phase Heat Transfer Enhancement in an Air-To-Water Heat Exchanger with Rectangular Perforated Flow Deflector Baffle Plate. *International Journal of Thermodynamics*, 26(4), 31–39. doi: 10.5541/ijot.1285385

[23] Rahman, M.A. (2023). The influence of geometrical and operational parameters on thermofluid performance of discontinuous colonial self-swirl-inducing baffle plate in a tubular heat exchanger. *Heat Transfer*, 53(2), 328-345. doi: 10.1002/htj.22956

[24] Rahman, M.A. (2023). Thermo-fluid performance comparison of an in-line perforated baffle with oppositely oriented rectangular-wing structure in turbulent heat exchanger. *International Journal of Fluid Mechanics Research*, 51(1), 15–30. doi: 10.1615/InterJFluidMechRes.2023051418

[25] Rahman, M.A. (2024). The effect of triangular shutter type flow deflector perforated baffle plate on the thermofluid performance of a heat exchanger. *Heat Transfer*, 53(2), 939–956. doi: 10.1002/htj.22981

[26] Habet, M.A., Ahmed, S.A., & Saleh, M.A. (2022). The effect of using staggered and partially tilted perforated baffles on heat transfer and flow characteristics in a rectangular channel. *International Journal of Thermal Sciences*, 174, 107422. doi: 10.1016/j.ijthermalsci.2021.107422

[27] Kumar, R., & Chandra, P. (2022). Experimental analysis to study the effect of perforated louvered strip-coiled spring insert on heat transfer performance in a double pipe heat exchanger. *Heat Transfer*, 51, 3035–056. doi: 10.1002/htj.22435

[28] Maithani, R., & Kumar, A. (2020). Effect of helical perforated twisted tape parameters on thermal and hydrodynamic performance in heat exchanger circular tube. *Heat and Mass Transfer*, 56, 507–519. doi: 10.1007/s00231-019-02716-9

[29] Veerabhadrappa B.M., Nagaraj, P.B., Lalagi, G., & Rajesh, K. (2023). Effect of triangular perforated flat cone-shaped inserts on performance of double-tube heat exchanger. *Physics of Fluids*, 35(11), 115133. doi: 10.1063/5.0169821

[30] Coleman, H. W., & Steele, W. G. (2018). *Experimentation, Validation, and Uncertainty Analysis for Engineers*. John Wiley & Sons.

[31] Cao, Y.Z. (1998). *Experimental Heat Transfer* (pp. 120–125). National Defence Industry Press, Beijing.

[32] Zhao, H., Wang, F., Wang, C., Chen, W., Yao, Z., Shi, X., & Zhong, Q. (2021). Study on the characteristics of horn-like vortices in an axial flow pump impeller under off-design conditions. *Engineering Applications of Computational Fluid Mechanics*, 15(1), 1613–1628. doi: 10.1080/19942060.2021.1985615